Mathematical and Computational Applications

MDPI

Article

An Application of Fractional Calculus to Column Theory

José Villa-Morales * and Manuel Ramírez-Aranda

Departamento de Matemáticas y Física, Universidad Autónoma de Aguascalientes, Av. Universidad No. 940, Aguascalientes 20100, Ags., Mexico

* Correspondence: j1v2m32004@gmail.com

Abstract

In this article, we employ a fractional version of the radius of curvature in Euler's equation for column buckling, enabling us to derive a fractional differential equation in the Caputo sense. We solve this equation and demonstrate that for certain values of the fractional parameter, there exists a critical buckling force. Additionally, we provide a numerical scheme for accurately approximating this critical force.

Keywords: Eulerian column theory; fractional differential equations; Caputo's derivative

1. Introduction

Although the origins of fractional calculus are quite old (around 1675), its theoretical development and, above all, its applications are relatively recent. See, for example, [1–4]. In many applications, fractional models are obtained by replacing the integer-order of the derivative in the original model with a fractional one. However, it has recently been observed that introducing an additional parameter, namely the fractional index, does not necessarily improve the resulting model; see [5–10]. Motivated by this observation, the purpose of the present work is to study the deflection of a column by deriving the governing fractional equation from a fractional approximation of the radius of curvature, rather than from a purely formal replacement of derivatives.

The analysis of buckling in materials, particularly in columns, is of crucial importance in applied mathematics and structural mechanics due to its numerous practical applications. This study is especially relevant in the construction industry, where the buckling of columns made from steel, aluminum, or plastic materials plays a key role. Similarly, this area of research is significant in other sectors, such as aviation and the automotive industries, among others. For further exploration of this topic, we refer the reader to [11–13] and the references therein.

Recent studies have shown that fractional calculus is not limited to abstract generalizations, but also provides useful tools in mechanics and structural stability. Fractional-order models have been used in continuum mechanics and materials modeling to describe nonlocal and size-dependent effects; see, for example, [14]. Moreover, fractional formulations have recently been applied to structural stability and buckling problems; see [15]. These works provide a relevant context for the present paper. In contrast with approaches based mainly on replacing classical derivatives with fractional ones, our model is obtained from a fractional approximation of the radius of curvature in Euler's column theory.

The main novelty of this work is therefore geometric in nature: the fractional model is derived from the curvature law itself. This construction leads to a Caputo-type fractional differential equation and provides a new analytical treatment of the buckling condition

Check for updates

Academic Editor: Gianluigi Rozza

Received: 28 May 2026
Revised: 7 July 2026
Accepted: 22 July 2026
Published: 1 August 2026

Copyright: © 2026 by the authors. Licensee MDPI, Basel, Switzerland. This article is an open access article distributed under the terms and conditions of the Creative Commons Attribution (CC BY) license.

through the first positive root of the associated solution. An important advantage of this formulation is that it extends the classical Euler model in a consistent way, recovers the standard case when $\alpha = 1$, and reveals a threshold behavior in the existence of the critical load that does not appear in the classical setting.

Suppose we have a beam of length l with one flexible end resting on the ground and a force P applied to the other flexible end. Under certain assumptions on the beam, the well-known Euler equation (see [16]) states that at a point x, the external moment $M(x)$ of the deflected beam is inversely proportional to the radius of curvature $\rho(x)$. symbols,

$$M(x) = \frac{EI}{\rho(x)}, \tag{1}$$

where E is the Young's modulus of the material and I denotes the second moment of inertia of the cross-sectional area. The displacement of the beam at point $x \in [0, l]$ is represented by $y(x)$, which corresponds to the elastic curve of the beam (refer to Figure 1).

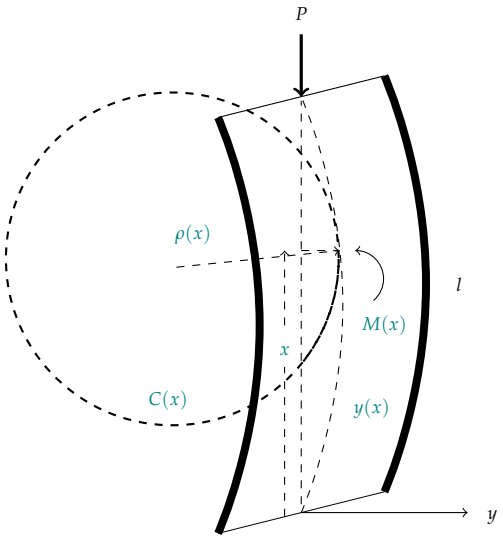


Figure 1. The elastic curve $y(\cdot)$ and the osculating circle $C(\cdot)$.

Assuming a scheme like the one presented in Figure 1, we know (see [17]) that the external moment is given by $M(x) = -P\,y(x)$. To introduce the fractional component, $\alpha \in (0, 1]$, into the study of beam deflection, we work with the radius of curvature, $\rho(x)$. Indeed, through a detailed analysis based on the Caputo fractional derivative and on a fractional approximation of the radius of curvature, as discussed in Section 2, we derive the fractional differential equation:

$$EI\left(\frac{\Gamma(2-\alpha)}{x^{1-\alpha}} \cdot D_{0+}^{1+\alpha} y(x)\right) = -P\,y(x), \quad x \in (0, l). \tag{2}$$

The fractional parameter $\alpha \in (0, 1]$ should be interpreted here as an effective index measuring the departure from the classical local Euler description. In the present formulation, α arises from the fractional approximation of the radius of curvature, so its most immediate meaning is geometric. The limiting case $\alpha = 1$ recovers the standard curvature law, whereas $0 < \alpha < 1$ introduces a nonclassical correction through a fractional curvature operator. Since this paper is conceptual and does not include experimental calibration, we do not assign α to a unique physical mechanism. Rather, it is treated as a compact parameter encoding nonlocal or nonclassical effects that are not captured by the ideal homogeneous Euler column model.

Currently, there is a wide variety of fractional derivatives available (see [18]). Among the classical ones are the Riemann-Liouville, Grünwald-Letnikov, Caputo, Riesz, and Marchaud derivatives, to name a few (see [19,20], or [21]). In this work, we adopt the Caputo derivative because the Caputo derivative of a constant is zero, which is consistent with the classical geometric interpretation underlying the model. Moreover, it allows the fractional differential equation to be formulated with standard initial conditions such as $y(0)$ and $y'(0)$, exactly as in the classical formulation. This makes the Caputo framework particularly suitable for deriving and analyzing the fractional counterpart of Euler's column equation considered here (see (15)).

The key point in our derivation is that, in the fractional setting, the classical differential increment cannot be transferred directly. Therefore, instead of postulating the fractional equation by replacing derivatives in Euler's model, we use a linear approximation of the arc $S(x)$ associated with the curvature radius $\rho(x)$, as indicated in (8). This procedure leads to the fractional model of column buckling considered in this paper.

The critical buckling force is given by

$$P_{\mathrm{cr}}(\alpha) = \frac{EI\,\Gamma(2-\alpha)}{l^2} \cdot s_{\mathbf{0}}(\alpha), \tag{3}$$

where $s_{\mathbf{0}}(\alpha)$ denotes the first positive zero of the solution $y(x)$ of Equation (2). In particular, if $\alpha = 1$ then $s_{\mathbf{0}} = \pi^2$, which coincides with the classical case (see [17]). Thus, the main complexity lies in the calculation of $s_{\mathbf{0}}$. According to our literature review, there are no precedents of studies that have identified positive roots for solutions of fractional differential equations in the Caputo context considered here. Beyond its practical motivation, this aspect of the work introduces analytical techniques that may also be useful in the study of solutions represented by power series.

To determine $s_{\mathbf{0}}$, or more precisely, to find an approximation of $s_{\mathbf{0}}$, we note that the function $y(x)$ is the uniform limit, over compact intervals, of certain polynomials. Assuming there is a polynomial $p_{n_{\mathbf{0}}}$ that meets specific conditions (see Assumption 1), we demonstrate that $y(x)$ has a positive root, as detailed in Theorem 2. Furthermore, if we impose additional regularity conditions on p_{n_0} (see Assumption 2), then for a given error ε, we can obtain an approximation of $s_{\mathbf{0}}$ that differs by less than ε units, as outlined in Theorem 3. Thus, we obtain an approximation of the critical force P, as seen in Equation (3).

Our numerical experiments suggest that $s_{\mathbf{0}}$ does not exist for all values of the index $\alpha \in (0, 1]$. Specifically, we observe that for $\alpha \leq 0.526$, the function $y(x)$ lacks positive roots, whereas the opposite occurs for $\alpha \geq 0.527$. This indicates a threshold phenomenon in the existence of the critical buckling force predicted by the fractional model. Additional qualitative features of the fractional solutions, including their symmetry properties and the possible use of

$$w(x) = \frac{y(x) + y(l-x)}{2}, \quad x \in [0, l],$$

are discussed in the numerical section.

The paper is structured as follows. In Section 2, we derive the radius of curvature involving the fractional index $\alpha \in (0, 1]$. In Section 3, Theorem 1 presents the solution $y(x)$ of Equation (2). Assuming that $y(x)$ can be approximated by a polynomial, we establish in Theorem 2 that $y(x)$ has a positive root. Additionally, Theorem 3 provides a method for approximating such a root. In Section 4, we demonstrate that for $\alpha = 0.526$, the function $y(x)$ does not have a positive root, whereas for $\alpha = 0.527$, it does. Finally, Section 5 contains some concluding comments.

2. A Fractional Approximation of the Radius of Curvature

Let us start by remembering the definition of the Caputo fractional derivative, for $\beta \in (0,\infty)\backslash\mathbb{N}$. The left-side Caputo fractional derivative of a smooth function $y : [0,l] \to \mathbb{R}$ is defined as

$$(D^{\beta}_{0+}y)(x) = \frac{1}{\Gamma(n-\beta)}\int_0^x \frac{y^{(n)}(t)}{(x-t)^{\beta-n+1}}dt,$$

where $n = [\beta]+1$ and $[\beta]$ denotes the integer part of β. It is known (see [21] or [20]) that Caputo's fractional derivative is linear and satisfies

$$(D^{\beta}_{0+}t^p)(x) = \begin{cases} 0, & p = 0,\ldots,n-1, \\ \frac{\Gamma(p+1)}{\Gamma(p+1-\beta)}x^{p-\beta}, & p > n-1. \end{cases} \tag{4}$$

Let us assume the function $y : [0,l] \to \mathbb{R}$ has second derivative. Given a point $x \in (0,l)$, we know that the radius of curvature, $\rho(x)$, of the osculating circle, $C(x)$, at $(x, y(x))$ is given by

$$\rho(x) = \frac{(1+(y'(x))^2)^{3/2}}{y''(x)}. \tag{5}$$

If the slope $y'(x)$ is small enough that its square can be disregarded compared to 1, then we have

$$\rho(x) \approx \frac{1}{y''(x)}. \tag{6}$$

The traditional derivation of the radius of curvature relies on differentials, a concept not directly translatable to the fractional realm. To approximate (6) in this context, we adopt the following approach. Let $\theta(x) \in (-\pi,\pi)$ such that $y'(x) = \tan\theta(x)$. Then, the equation

$$L(z) = y(x) + y'(x)(z-x), \ \ z \in (0,l),$$

describes the tangent line to y at the point $P = (x, y(x))$. Now, consider a point z close to x, and suppose, for example, $z < x$. Denote by $\theta(z)$ the angle between the segments associated with z and x, and denote by $T(z)$ the tangent line at $(z, C(z))$ on the osculating circle (see Figure 2).

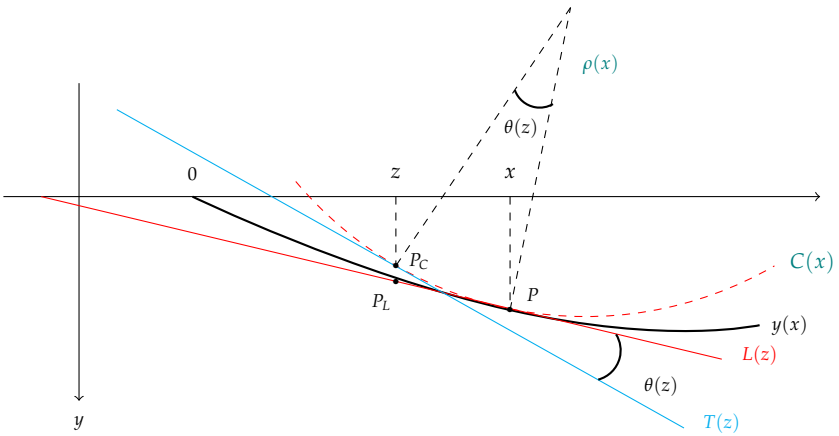


Figure 2. The osculating circle $C(x)$.

Let us denote by $S(z)$ the length of the arc corresponding to a circle with angle $\theta(z)$ and by $\rho(x)$ the radius of curvature at x, then

$$S(z) = \rho(x)\theta(z), \ \ z \in (0,l). \tag{7}$$

We adhere to the convention of considering the angle positive if it is measured in the clockwise direction. If z approaches x from the left, then $\theta(z)$ is negative. Given that z is close to x, the points $P_C = (z, C(z))$ and $P_L = (z, L(z))$ are nearly coincident. Consequently, the magnitude of $S(z)$ is approximately the length of the segment from $P_L = (z, L(z))$ to $P = (x, y(x))$:

$$\begin{aligned} S(z) &\approx \begin{cases} -\sqrt{(z-x)^2 + (L(z) - y(x))^2}, & 0 < z < x, \\ \sqrt{(z-x)^2 + (L(z) - y(x))^2}, & x < z < l. \end{cases} \\ &= \sqrt{1 + (y'(x))^2} \cdot (z - x). \end{aligned} \tag{8}$$

Utilizing the linearity property of Caputo's fractional derivative and referencing Equation (4), with $0 < \alpha < 1$, $\beta = 1$, and $n = 1$, we derive

$$\begin{aligned} D^{\alpha}_{0+} S(z) &\approx \sqrt{1 + (y'(x))^2}\, D^{\alpha}_{0+}(z - x) \\ &= \frac{\sqrt{1 + (y'(x))^2}}{\Gamma(2 - \alpha)} \cdot z^{1-\alpha}. \end{aligned} \tag{9}$$

Now, let us focus on the right-hand side of (7), specifically addressing the function $\theta(z)$. Let $\theta(x) = \tan^{-1}(y'(x))$ be the angle of the line L. Drawing a line parallel to the x-axis that passes through the point I, where the lines L and T intersect, we see that the angle of line T is $\theta(x) + \theta(z)$. Let R be the tangent line at the point $P_z = (z, y(z))$,

$$R(w) = y(z) + y'(z)(w - z), \quad w \in (0, l).$$

Since $z \approx x$ and because the elastic curve $y(\cdot)$ is a smooth function, then $P_z \approx P_C$. Moreover, the angle of line T is approximately equal to the angle of line R (see Figure 3):

$$\theta(x) + \theta(z) \approx \tan^{-1}(y'(z)). \tag{10}$$

Since $z \approx x$, then $\theta(z) \approx 0$. We know that for small angles x, given in radians, $x \approx \tan x$. Using this and (10) we deduce that

$$\theta(x) + \theta(z) \approx \tan(\theta(x) + \theta(z)) \approx y'(z). \tag{11}$$

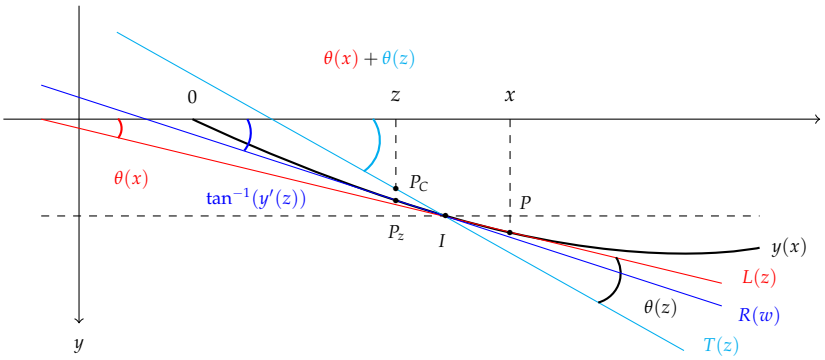


Figure 3. The tangent lines. In blue is the tangent line $R(w)$ at $(z, y(z))$.

The observation that the fractional derivative of constant functions is zero, as indicated in Equation (4), results in the following equation

$$D^{\alpha}_{0+}\theta(z) = D^{\alpha}_{0+}(\theta(x) + \theta(z)) \approx D^{\alpha}_{0+} y'(z) = D^{\alpha+1}_{0+} y(z). \tag{12}$$

At this stage, x is regarded as an arbitrary but fixed point, and the fractional differentiation is taken with respect to the auxiliary variable z. Therefore, in the identity

$$S(z) = \rho(x)\theta(z),$$

the quantity $\rho(x)$ is constant with respect to z. Evaluating the resulting relation at $z = x$, we obtain

$$D_{0+}^{\alpha} S(z)\big|_{z=x} = \rho(x)\, D_{0+}^{\alpha}\theta(z)\big|_{z=x}.$$

Applying (9) and (12), we can deduce an analogue of (5),

$$\rho(x) = \frac{x^{1-\alpha}}{\Gamma(2-\alpha)} \cdot \frac{(1+(y'(x))^2)^{1/2}}{D_{0+}^{\alpha+1} y(x)}.$$

As in the previous case, if the square of $y'(x)$ is significantly smaller than 1, we arrive at the approximation

$$\rho(x) \approx \frac{x^{1-\alpha}}{\Gamma(2-\alpha)} \cdot \frac{1}{D_{0+}^{\alpha+1} y(x)}. \tag{13}$$

This is similar to (6), but with the additional factor of $x^{1-\alpha}/\Gamma(2-\alpha)$.

3. Solving the Fractional Differential Equation

For $\alpha \in (0, 1]$, we define the parameter λ as follows

$$\lambda := \frac{P}{EI\,\Gamma(2-\alpha)},$$

where E, I and P are positive constants. Our first aim is to solve the fractional differential equation

$$D_{0+}^{1+\alpha} y(x) = -\lambda x^{1-\alpha}\, y(x), \tag{14}$$

subject to the initial conditions

$$y(0) = b_0, \quad y'(0) = b_1. \tag{15}$$

An intuitive way to understand the influence of the fractional order is the following. The parameter α changes the structure of the differential operator in Equation (14), and hence changes the series representation of the solution $y(x)$. This affects the way in which the solution bends and approaches the horizontal axis. Therefore, unlike in the classical case, the existence of a first positive zero is no longer automatic and may depend strongly on the value of α. As we will see, this explains why the critical buckling load exists only for certain ranges of the fractional parameter.

Given the physical constraints of the problem, we have $b_0 = 0$. The initial condition for the derivative, denoted as b_1, remains undetermined. Identifying b_1 is crucial for calculating the critical load. We start by seeking the solution to the initial value problem (14) and (15).

Theorem 1. *Let us set*

$$y(x) = b_1 \left(a_0\, x + \sum_{k=1}^{\infty} (-1)^k a_k \lambda^k x^{2k+1} \right), \quad x \in \mathbb{R}, \tag{16}$$

where

$$a_0 := 1, \quad a_k := \prod_{i=1}^{k} \frac{\Gamma(2i+1-\alpha)}{\Gamma(2i+2)}, \quad k \in \mathbb{N}.$$

The series converges absolutely and represents the solution to the initial value problem as stated in Equations (14) and (15).

Proof. By applying the root criterion, we can ascertain that the power series in (16) converges absolutely over $\mathbb{R}$. This conclusion is drawn from the observation that

$$\limsup_{k\to\infty}\left(|(-1)^k a_k|\right)^{1/k} \leq \limsup_{k\to\infty}\frac{|(-1)^{k+1}a_{k+1}|}{|(-1)^k a_k|} = \limsup_{k\to\infty}\frac{\Gamma(2k+3-\alpha)}{\Gamma(2k+4)} = 0.$$

On the other hand, given that $y(0) = 0$ and

$$y'(x) = b_1\left(1 + \sum_{k=1}^{\infty}(-1)^k a_k \lambda^k (2k+1)x^{2k}\right),$$

yield $y'(0) = b_1$. Now, let us calculate the fractional derivative of $y(x)$,

$$D_{0+}^{\alpha+1}y(x) = b_1\left(D_{0+}^{\alpha+1}x + \sum_{k=1}^{\infty}(-1)^k a_k \lambda^k D_{0+}^{\alpha+1}x^{2k+1}\right).$$

Since $\alpha+1 \in (1,2]$, then $D_{0+}^{\alpha+1}x = 0$ (see (4)). Furthermore, for $k \geq 1$,

$$D_{0+}^{\alpha+1}x^{2k+1} = \frac{\Gamma(2k+2)}{\Gamma(2k+1-\alpha)}x^{2k-\alpha},$$

from which we derive

$$\begin{aligned} D_{0+}^{\alpha+1}y(x) &= b_1\sum_{k=1}^{\infty}(-1)^k a_k \lambda^k \frac{\Gamma(2k+2)}{\Gamma(2k+1-\alpha)}x^{2k-\alpha} \\ &= b_1\left(-\lambda x^{2-\alpha} + \sum_{k=2}^{\infty}(-1)^k a_{k-1}\lambda^k x^{2k-\alpha}\right) \\ &= -\lambda x^{1-\alpha} b_1\left(x + \sum_{k=1}^{\infty}(-1)^k a_k \lambda^k x^{2k+1}\right) \\ &= -\lambda x^{1-\alpha} y(x). \end{aligned}$$

This result confirms the desired equality (14). □

For $n \in \mathbb{N}\cup\{\infty\}$ we define

$$p_n(x) = \sum_{k=0}^{n}(-1)^k a_k x^k, \quad x \in \mathbb{R}.$$

Then the solution $y(x)$ of (14) can be expressed as

$$y(x) = b_1 x p_\infty(\lambda x^2), \quad x \in [0, l].$$

We know that $y(l) = 0$, then $b_1 = 0$ or $p_\infty(\lambda l^2) = 0$. If $b_1 = 0$, the column has not bent at all. On the other hand we have $p_\infty(\lambda l^2) = 0$. Thus we need to find the smallest positive root of the function p_∞ in order to obtain the critical load (force).

We denote the smallest positive root of the polynomial p_n as r_n. The existence of r_n depends on whether n is an odd or even integer. For odd integers n, a root r_n always exists. This is due to the intermediate value theorem, as a polynomial of odd degree must cross the x-axis at least once, ensuring at least one real root. However, for even integers n, the existence of such a root is not guaranteed.

Lemma 1. *Let α be in $(0,1]$. The following functions defined on $\mathbb{N}$*

$$f(x) = \frac{\Gamma(x+1)}{\Gamma(x-\alpha)},$$
$$g(x) = \frac{x\Gamma(2x+4)}{(x+1)\Gamma(2x+3-\alpha)},$$

are both $f(x)$ and $g(x)$ strictly increasing functions.

Proof. To verify the monotonicity property, we will use the relation $\Gamma(x+1) = x\Gamma(x)$ for $x \in (0,\infty)$. Applying this, we have

$$\begin{aligned}\frac{\Gamma(x+2)}{\Gamma(x+1-\alpha)} &= \frac{(x+1)\Gamma(x+1)}{(x-\alpha)\Gamma(x-\alpha)}\\ &\geq \frac{x+1}{x}\cdot\frac{\Gamma(x+1)}{\Gamma(x-\alpha)}\\ &= \left(1+\frac{1}{x}\right)\cdot\frac{\Gamma(x+1)}{\Gamma(x-\alpha)}\\ &> \frac{\Gamma(x+1)}{\Gamma(x-\alpha)}\end{aligned}$$

and

$$\begin{aligned}\frac{x+1}{x+2}\cdot\frac{\Gamma(2x+6)}{\Gamma(2x+5-\alpha)} &= \frac{(x+1)^2(2x+5)(2x+4)}{x(x+2)(2x+4-\alpha)(2x+3-\alpha)}\cdot\frac{x\Gamma(2x+4)}{(x+1)\Gamma(2x+3-\alpha)}\\ &\geq \frac{(x+1)^2(2x+5)}{x(x+2)(2x+3)}\cdot\frac{x\Gamma(2x+4)}{(x+1)\Gamma(2x+3-\alpha)}\\ &= \left(1+\frac{2x+5}{2x^3+9x^2+10x}\right)\cdot\frac{x\Gamma(2x+4)}{(x+1)\Gamma(2x+3-\alpha)}\\ &> \frac{x\Gamma(2x+4)}{(x+1)\Gamma(2x+3-\alpha)}.\end{aligned}$$

Thus, the desired property is clearly established. □

In what follows we require the following hypothesis.

Assumption 1. *Let us suppose there is a polynomial p_{n_0}, with n_0 an even integer, such that it has a first positive root r_{n_0} that satisfies the inequality*

$$\frac{\Gamma(2n_0+6)}{\Gamma(2n_0+5-\alpha)} \geq r_{n_0}.$$

Lemma 2. *For each $n, m \in \mathbb{N}\cup\{0\}$ we have $p_{n_0+2n+1} < p_\infty < p_{n_0+2m}$ on $(0, r_{n_0}]$.*

Proof. Given that the series below converges absolutely, we can rearrange the terms as follows

$$\begin{aligned}p_\infty(x) - p_{n_0+2n+1}(x) &= \sum_{k=n_0+2n+2}^{\infty}(-1)^k a_k x^k\\ &= \sum_{k=0}^{\infty} a_{n_0+2n+2k+2}\, x^{n_0+2n+2k+2} - \sum_{k=0}^{\infty} a_{n_0+2n+2k+3}\, x^{n_0+2n+2k+3}\\ &= \sum_{k=0}^{\infty} a_{n_0+2n+2k+2}\, x^{n_0+2n+2k+2}\left(1-\frac{\Gamma(2n_0+4n+4k+7-\alpha)}{\Gamma(2n_0+4n+4k+8)}x\right).\end{aligned}$$

https://doi.org/10.3390/mca31040148

The monotonicity property of f, as stated in Lemma 1, and the condition $x \in (0, r_{n_0}]$ imply

$$\frac{\Gamma(2n_0+4n+4k+8)}{\Gamma(2n_0+4n+4k+7-\alpha)} \geq \frac{\Gamma(2n_0+8)}{\Gamma(2n_0+7-\alpha)} > \frac{\Gamma(2n_0+6)}{\Gamma(2n_0+5-\alpha)} \geq r_{n_0} \geq x,$$

therefore, $p_\infty > p_{n_0+2n+1}$ on $(0, r_{n_0}]$.

Now, let us consider

$$p_\infty(x) - p_{n_0+2m}(x) = \sum_{k=0}^{\infty} a_{n_0+2m+2k+1}\, x^{n_0+2m+2k+1} \left(\frac{\Gamma(2n_0+4m+4k+5-\alpha)}{\Gamma(2n_0+4m+4k+6)} x - 1 \right).$$

For $k \geq 1$ and $x \in (0, r_{n_0}]$, Lemma 1 implies

$$\frac{\Gamma(2n_0+4m+4k+6)}{\Gamma(2n_0+4m+4k+5-\alpha)} > \frac{\Gamma(2n_0+6)}{\Gamma(2n_0+5-\alpha)} \geq r_{n_0} \geq x,$$

thus $p_{n_0+2m} > p_\infty$ on $(0, r_{n_0}]$. This completes the proof of the desired inequalities. □

We now turn our attention to a result concerning the monotonicity of the sequence $(p_n)_{n\in\mathbb{N}}$. This investigation will help us understand how the sequence behaves as n varies, particularly in terms of its increasing or decreasing nature.

Lemma 3. *Let n and m be two positive integers such that $n > m$. If m and n are even integers, then $p_{n_0+n} < p_{n_0+m}$ on $(0, r_{n_0}]$. Additionally, if m and n are odd integers, then $p_{n_0+n} > p_{n_0+m}$ on $(0, r_{n_0}]$.*

Proof. If n and m are even integers, with $n > m$, then

$$\begin{aligned} p_{n_0+n}(x) - p_{n_0+m}(x) &= \sum_{k=n_0+m+1}^{n_0+n} (-1)^k a_k x^k \\ &= \sum_{k=0}^{(n-m-2)/2} a_{2k+n_0+m+1}\, x^{2k+n_0+m+1} \left(\frac{\Gamma(2n_0+2m+4k+5-\alpha)}{\Gamma(2n_0+2m+4k+6)} x - 1 \right). \end{aligned}$$

For $x \in (0, r_{n_0}]$ we have, from Lemma 1,

$$\frac{\Gamma(2n_0+2m+4k+6)}{\Gamma(2n_0+2m+4k+5-\alpha)} \geq \frac{\Gamma(2n_0+10)}{\Gamma(2n_0+9-\alpha)} > \frac{\Gamma(2n_0+6)}{\Gamma(2n_0+5-\alpha)} \geq r_{n_0} \geq x.$$

Therefore $p_{n_0+m} > p_{n_0+n}$ on $(0, r_{n_0}]$.

Now, let m and n be two odd integers such that $n > m$, then

$$p_{n_0+n}(x) - p_{n_0+m}(x) = \sum_{k=0}^{(n-m-2)/2} a_{n_0+2k+m+1}\, x^{n_0+2k+m+1} \left(1 - \frac{\Gamma(2n_0+4k+2m+5-\alpha)}{\Gamma(2n_0+4k+2m+6)} x \right).$$

Again, by Lemma 1 we have, for $x \in (0, r_{n_0}]$,

$$\frac{\Gamma(2n_0+4k+2m+6)}{\Gamma(2n_0+4k+2m+5-\alpha)} \geq \frac{\Gamma(2n_0+10)}{\Gamma(2n_0+9-\alpha)} > \frac{\Gamma(2n_0+6)}{\Gamma(2n_0+5-\alpha)} \geq r_{n_0} \geq x,$$

therefore $p_{n_0+m} < p_{n_0+n}$ on $(0, r_{n_0}]$. This proves the result. □

Note that $p_{n_0+1}(0) = 1$ and

$$p_{n_0+1}(r_{n_0}) = p_{n_0}(r_{n_0}) - a_{n_0+1}\, x^{n_0+1} < 0,$$

since $p_{n_0}(r_{n_0}) = 0$. Therefore, by the intermediate value theorem, there exists a root r_{n_0+1} such that $0 < r_{n_0+1} < r_{n_0}$. We are now equipped to demonstrate the existence of a positive root for p_∞.

Theorem 2. *The function p_∞ has a first positive root, and this root is located in (r_{n_0+1}, r_{n_0}).*

Proof. By taking $m = 0$ in Lemma 2, we deduce that $p_\infty(r_{n_0}) < p_{n_0}(r_{n_0}) = 0$. Given that $p_\infty(0) = 1$, the intermediate value theorem guarantees that p_∞ must have a root in the interval $(0, r_{n_0})$. Let us denote by $s_{\mathbf{0}}$ the first positive root of p_∞.

For each $n \in \mathbb{N} \cup \{0\}$, Lemma 2 implies that $p_{n_0+2n+1}(s_{\mathbf{0}}) < p_\infty(s_{\mathbf{0}}) = 0$. Therefore, p_{n_0+2n+1} has a root r_{n_0+2n+1}, and it follows that $r_{n_0+2n+1} < s_{\mathbf{0}}$. Consequently, we obtain a sequence $(r_{n_0+2n+1})_{n\in\mathbb{N}\cup\{0\}}$. This sequence is increasing; indeed, Lemma 3 indicates that $p_{n_0+2n+1}(r_{n_0+2n+3}) < p_{n_0+2n+3}(r_{n_0+2n+3}) = 0$, implying that $r_{n_0+2n+1} < r_{n_0+2n+3}$. Let us define

$$r := \lim_{n\to\infty} r_{n_0+2n+1} = \sup_{n\in\mathbb{N}\cup\{0\}} \{r_{n_0+2n+1}\} \leq s_{\mathbf{0}}.$$

We aim to show that $r = s_{\mathbf{0}}$. To do this, suppose that $r < s_{\mathbf{0}}$. Take an $\tilde{r} \in (r, s_{\mathbf{0}})$. By the definition of $s_{\mathbf{0}}$ we have $p_\infty(x) > 0$ for $x \in [r_{n_0+1}, \tilde{r}]$. The continuity of p_∞ implies

$$\min_{z\in[r_{n_0+1},\tilde{r}]} \{p_\infty(z)\} > 0.$$

By Weierstrass's M-test, the sequence $(p_n)_{n\in\mathbb{N}}$ converges uniformly over compact intervals. Hence, there exists $n_1 \in \mathbb{N}$ such that for all $n \geq n_1$,

$$|p_\infty(x) - p_n(x)| < \frac{1}{2} \min_{z\in[r_{n_0+1},\tilde{r}]} \{p_\infty(z)\}, \quad x \in [r_{n_0+1}, \tilde{r}].$$

In particular, we can choose a sufficiently large odd integer n such that $r_n \in (r_{n_0+1}, r)$. The preceding inequality then leads to

$$0 = p_n(r_n) > \frac{1}{2}\, p_\infty(r_n) > 0.$$

This contradiction implies the desired equality, $r = s_{\mathbf{0}}$. □

We now propose a method to approximate the first positive root of p_∞. To this end, we introduce the following hypothesis.

Assumption 2. *We assume that $p'_{n_0}(x) \leq 0$ for x on $[r_{n_0+1}, r_{n_0}]$ and that*

$$\frac{n_0+1}{n_0+2} \cdot \frac{\Gamma(2n_0+6)}{\Gamma(2n_0+5-\alpha)} \geq r_{n_0}.$$

Theorem 3. *If $n \geq n_0$, regardless of whether n is even or odd, the existence of the first root, r_n, of p_n is guaranteed. Furthermore, the sequence $(r_n)_{n\in\mathbb{N}}$ satisfies the condition*

$$\lim_{n\to\infty} (r_{n+1} - r_n) = 0. \tag{17}$$

Given an $\varepsilon > 0$ we can find an integer $\tilde{n}$ (existence ensured by the first part of this theorem) such that

$$|r_{\tilde{n}} - r_{\tilde{n}+1}| < \varepsilon \tag{18}$$

then

$$|s_{\mathbf{0}} - r_{\tilde{n}}| < \varepsilon. \tag{19}$$

Consequently, this provides an approximation to the first positive root, s_0, of p_∞ with an error margin of at most ε units.

Proof. For each $m \in \mathbb{N} \cup \{0\}$, we have $p_{n_0+2m}(0) = 1$. Note that Lemma 3 implies $p_{n_0+2m}(r_{n_0}) < p_{n_0}(r_{n_0}) = 0$. Therefore, p_{n_0+2m} has a minimal positive root, r_{n_0+2m}, for all $m \in \mathbb{N} \cup \{0\}$. Additionally, Lemma 2 indicates that $p_\infty(x) < p_{n_0+2m}(x)$ in $(0, r_{n_0}]$ and since $p_\infty(s_0) = 0 < p_{n_0+2m}(s_0)$, it follows that $s_0 < r_{n_0+2m}$. Furthermore, according to Lemma 3 we have $p_{n_0+2m+2}(r_{n_0+2m}) < p_{n_0+2m}(r_{n_0+2m}) = 0$, implying $r_{n_0+2m+2} < r_{n_0+2m}$. Consequently, the sequence $(r_{n_0+2m})_m$ is monotonically decreasing and bounded below by s_0. This leads to the conclusion that

$$r := \lim_{m\to\infty} r_{n_0+2m} = \inf_{m\in\mathbb{N}\cup\{0\}} \{r_{n_0+2m}\} \geq s_0.$$

Now, let us demonstrate that $s_0 = r$. Suppose, for contradiction, that $s_0 < r$. First, let us consider the expression

$$p'_\infty(x) - p'_{n_0}(x) = \sum_{k=0}^{\infty} a_{n_0+2k}\, x^{n_0+2k+1} \left((n_0+2k+2) \frac{\Gamma(2n_0+4k+5-\alpha)}{\Gamma(2n_0+4k+6)} x - (n_0+2k+1) \right).$$

Using the monotonicity property of g as established in Lemma 1, for $x \in (0, r_{n_0}]$ and $k \geq 1$, we have

$$\frac{n_0+2k+1}{n_0+2k+2} \cdot \frac{\Gamma(2n_0+4k+6)}{\Gamma(2n_0+4k+5-\alpha)} > \frac{n_0+1}{n_0+2} \cdot \frac{\Gamma(2n_0+6)}{\Gamma(2n_0+5-\alpha)} \geq r_{n_0} \geq x,$$

which implies that $p'_\infty(s_0) < p'_{n_0}(s_0) \leq 0$. The continuity of p'_∞ implies the existence of a $\delta > 0$ such that $p_\infty(x) < p_\infty(s_0) = 0$, for all $s_0 \leq x < s_0 + \delta < r$. Let us take an $\tilde{x} \in (s_0, s_0 + \delta)$. Since $\lim_{n\to\infty} p_n(\tilde{x}) = p_\infty(\tilde{x})$ we can find a large enough even integer n such that

$$|p_\infty(\tilde{x}) - p_n(\tilde{x})| < -p_\infty(\tilde{x}),$$

which implies that $p_n(\tilde{x}) < 0$. Given that $p_n(0) = 1$ and by applying the intermediate value theorem, it follows that $r_n < s_0 + \delta < r$. However, this conclusion is contradictory, as we have established that $r \leq r_n$ for all even integer n. Consequently, it must be that $s_0 = r$.

Given $\varepsilon > 0$, there exists an integer $\tilde{n}$, such that if $i \geq \tilde{n}$ and $j \geq \tilde{n}$, with i an odd integer and j an even integer, then

$$|r_i - s_0| < \frac{\varepsilon}{2}, \quad |r_j - s_0| < \frac{\varepsilon}{2}.$$

Consequently, if $n \geq \tilde{n}$, we have

$$|r_{n+1} - r_n| < |r_{n+1} - s_0| + |r_n - s_0| < \varepsilon.$$

Thus, the limit as expressed in (17) is effectively established. □

In this context, we have found an approximation, $r_{\tilde{n}}$, of s_0. Therefore, if $p_\infty(\lambda l^2) = 0$, it follows that

$$\frac{P}{EI\,\Gamma(2-\alpha)}\, l^2 = s_0.$$

From this, we obtain an approximate critical load, see the Formula (3).

Assumptions 1 and 2 are analytical and numerical admissibility conditions on the polynomial approximations p_n, not physical hypotheses on the material. Together, they ensure that the first positive root of the limit function p_∞ can be detected and approximated from the roots of suitable truncations.

Assumption 1 requires an even-degree truncation p_{n_0} to possess a first positive root r_{n_0} satisfying a quantitative inequality. This guarantees that the truncation captures the relevant sign change, which is essential for proving that p_∞ admits a root in the interval(r_{n_0+1}, r_{n_0}).

Assumption 2 complements this with a local monotonicity condition on p'_{n_0} over $[r_{n_0+1}, r_{n_0}]$ and an additional quantitative bound. Jointly, these conditions ensure the numerical stability of the truncated roots and enable Theorem 3 to deliver a controlled approximation of s_0. In short, Assumptions 1 and 2 are practical criteria ensuring that the truncation is sufficiently faithful near the root of interest, as the next section makes clear.

4. Some Illustrative Examples

In this section, we explore two illustrative examples that clarify the concepts. It should be noted that the approximation of the first positive root s_0 is performed in two steps. First, Theorem 3 provides the theoretical approximation criterion: given $\varepsilon > 0$, an index $\tilde{n}$ is chosen such that

$$|r_{\tilde{n}+1} - r_{\tilde{n}}| < \varepsilon,$$

which guarantees that

$$|s_0 - r_{\tilde{n}}| < \varepsilon.$$

Therefore, calculating the first positive root s_0 of p_∞ using the first positive root $r_{\tilde{n}}$ of the polynomial $p_{\tilde{n}}$ already has an explicit error bound.

Once the polynomial $p_{\tilde{n}}$ is fixed, its first positive root $r_{\tilde{n}}$ is calculated numerically using the bisection method. The continuity of the polynomial $p_{\tilde{n}}$ implies that the bisection method is convergent. Furthermore, in each iteration, the interval containing the root is halved, so the midpoint approximation is numerically stable and its error is controlled by the length of the current interval.

In our implementation, the calculation ended when the numerical value of the root stabilized on the order of 10^{-5}. In this way, the overall approximation of s_0 combines the theoretical estimate provided by Theorem 3 with the numerical precision of the bisection routine.

4.1. Non-Existence of an Even Degree Polynomial P_{N_0} with a Positive Root

In this subsection, we will take $\alpha = 0.526$ and $n \in \mathbb{N} \cup \{0\}$. Observe that

$$p_\infty(x) - p_{2n+1}(x) = \sum_{k=0}^{\infty} a_{2n+2k+2}\, x^{2n+2k+2}\left(1 - \frac{\Gamma(4n+4k+6.474)}{\Gamma(4n+4k+8)}x\right).$$

According to Lemma 1, for $k \geq 1$,

$$\frac{\Gamma(4n+4k+8)}{\Gamma(4n+4k+6.474)} > \frac{\Gamma(4n+8)}{\Gamma(4n+6.474)},$$

therefore, $p_\infty > p_{2n+1}$ on $[0, \Gamma(4n+8)/\Gamma(4n+6.474)]$. This particularly implies that if

$$r_{2n+1} \in [0, \Gamma(4n+8)/\Gamma(4n+6.474)], \tag{20}$$

then p_∞ does not have a root in $[0, r_{2n+1}]$.

The Table 1 displays the first positive root r_m of the polynomial p_m along with the corresponding evaluation of the term $\Gamma(2m+6)/\Gamma(2m+4.474)$.

Table 1. First positive root r_m of the odd-degree polynomial p_m for selected values of m, together with the corresponding value of $\Gamma(2m+6)/\Gamma(2m+4.474)$. The comparison shows that r_m remains below this bound in every case listed, thereby verifying condition (20) for $\alpha = 0.526$ and supporting the numerical evidence that p_∞ has no positive root in this regime.

p_m	p_1	p_3	p_5	p_7	p_9	p_{11}	p_{13}	p_{15}	p_{17}	p_{19}	p_{21}
r_m	4.56	7.93	11.31	14.37	16.68	29.93	38.25	46.25	54.5	63.31	72.87
$\frac{\Gamma(2m+6)}{\Gamma(2m+4.474)}$	18.3	37.3	60.6	87.5	117.5	150.5	186.2	224.5	265.1	308.0	353.1

From Table 1, we observe that the condition (20) is fulfilled in each instance. Consequently, it can be inferred that p_∞ has no roots within the interval $[0, r_m]$. Moreover, we notice that the root r_m increases with the degree m of the odd polynomial p_m. This observation, in conjunction with the graph of p_∞ presented in Figure 4, provides numerical evidence supporting the conclusion that p_∞ lacks a positive root when $\alpha = 0.526$. In fact, for values of α less than 0.526, the function p_∞ also appears to be devoid of positive roots, as exemplified by the graphs of p_∞ in Figure 5, corresponding to $\alpha = 0.1$ and $\alpha = 0.4$.

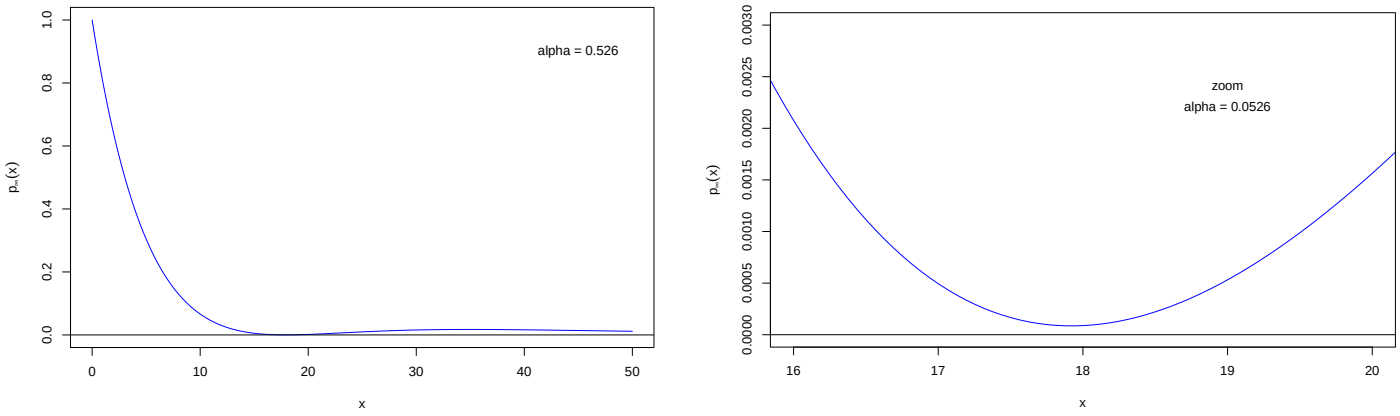


Figure 4. Plot of $p_\infty(x)$ for $\alpha = 0.526$ as a function of the dimensionless argument x. The right panel shows a zoom near the minimum. Since the curve remains positive and does not cross the horizontal axis, no positive root is detected in this threshold case. Consequently, the fractional model does not predict a critical buckling load at $\alpha = 0.526$.

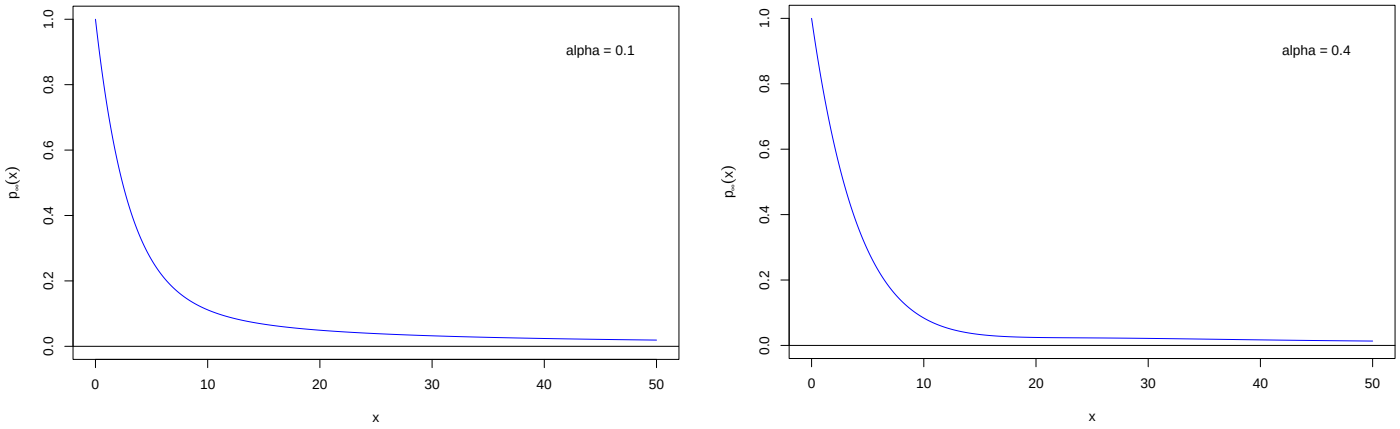


Figure 5. Plots of $p_\infty(x)$ for $\alpha = 0.1$ and $\alpha = 0.4$ versus the dimensionless argument x. In both cases the function stays above zero over the plotted interval, providing numerical evidence that no positive root exists for these values of α. From the mechanical viewpoint, this indicates that the present fractional model does not yield a critical buckling load in this regime.

4.2. Existence of an Even Degree Polynomial P_{N_0} with a Positive Root

Now, we will consider $\alpha = 0.527$. Polynomials p_2, p_4, p_6, p_8 and p_{10} do not have positive roots. However, polynomial p_{12} does have a positive root, $r_{12} \approx 17.31$, as shown in Figure 6. Let us set $n_0 = 12$. Then

$$168.65 \approx \frac{\Gamma(2n_0+5)}{\Gamma(2n_0+5-\alpha)} \geq r_{n_0} \approx 17.31. \tag{21}$$

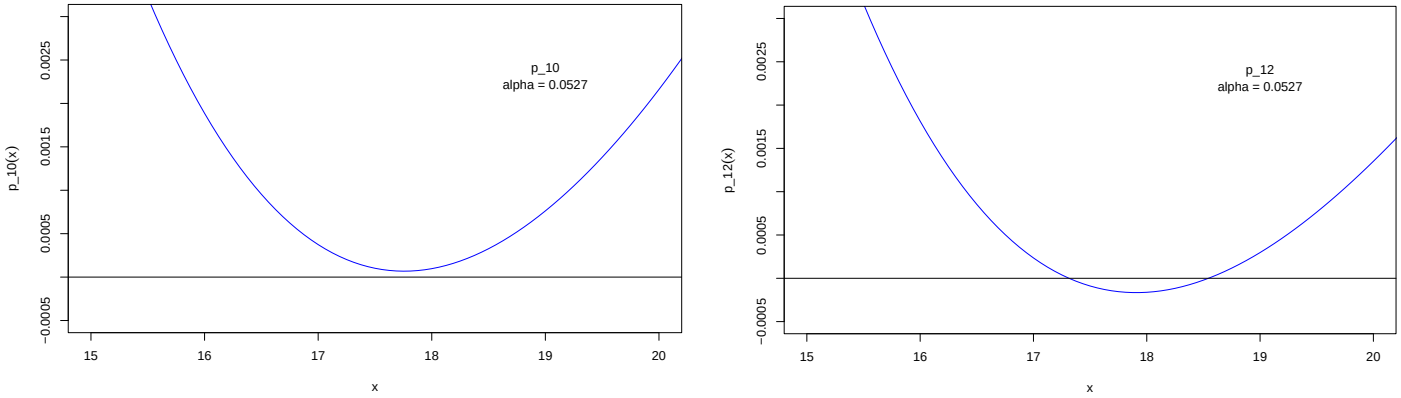


Figure 6. Plots of the truncation polynomials $p_{10}(x)$ and $p_{12}(x)$ for $\alpha = 0.527$, shown against the dimensionless argument x. While p_{10} does not exhibit a positive zero, p_{12} crosses the horizontal axis near $x \approx 17.31$, indicating the appearance of a positive root. This marks the onset of the regime in which the fractional model predicts a critical buckling load.

The Table 2 presents the roots of the polynomials p_{12}, p_{13}, p_{14} and p_{15} for various values of α.

Table 2. First positive roots of the truncation polynomials p_{12}, p_{13}, p_{14}, and p_{15} for $\alpha = 0.527$, $\alpha = 0.6$, and $\alpha = 0.7$. For $\alpha = 0.527$, the closeness of the values r_{12}, r_{13}, r_{14}, and r_{15} numerically confirms the localization of the first positive root of p_∞ in a short interval near 17.31. For $\alpha = 0.6$ and $\alpha = 0.7$, the near coincidence of the listed roots shows that the sequence stabilizes rapidly as α increases, so that the root of p_{12} already gives an excellent approximation of the first positive root of p_∞.

r_m \ α	**0.527**	**0.6**	**0.7**
r_{12}	17.31407406	12.97715575	11.45145303
r_{13}	17.30910486	12.97715515	11.45145302
r_{14}	17.30961111	12.97715518	11.45145302
r_{15}	17.30956418	12.97715518	11.45145302

From this, we observe that $r_{n_0+1} \approx 17.3$. The inequality (21) confirms that Assumption 1 is satisfied. Consequently, based on Theorem 1, it follows that the first positive root of p_∞ lies within the interval $(17.3, 17.31)$.

Now, let's assume we aim to find the root of p_∞ with an error margin less than $\varepsilon = 1 \times 10^{-3}$. To achieve this, it is necessary to ensure that Assumption 2 is fulfilled. Observing the graph of p_{12} (see Figure 6) we can infer that p_{12} is decreasing in the interval $(16, 17.5)$. Consequently, $p'_{12} < 0$ on $[r_{13}, r_{12}] \approx [17.3, 17.31]$, and

$$156.6 \approx \frac{n_0+1}{n_0+2} \cdot \frac{\Gamma(2n_0+6)}{\Gamma(2n_0+5-\alpha)} \geq r_{n_0} \approx 17.31,$$

thus Assumption 2 is satisfied. Recall that $\alpha = 0.527$ and

$$|r_{14} - r_{15}| = 4.693 \times 10^{-5} < 1 \times 10^{-3},$$

which, according to Theorem 2, implies that

$$|s_0 - r_{14}| < 1 \times 10^{-3}.$$

Therefore, $r_{14} = 17.30961111$ serves as the desired approximation.

The numerical computations presented in this section indicate that p_∞ possesses a positive root for the sample values $\alpha = 0.527, 0.6$, and 0.8, whereas no positive root is detected for $\alpha = 0.526, 0.4$, and 0.1. Therefore, within the numerical evidence considered here, the transition between non-existence and existence of a positive root appears to occur near $\alpha \approx 0.526$–0.527, see in Figure 7. Additionally, Table 2 illustrates that the root r_m tends to stabilize rapidly with increasing values of α. Consequently, the root of p_{12} serves as an excellent approximation for the root of p_∞ when α is greater than 0.6 or 0.7.

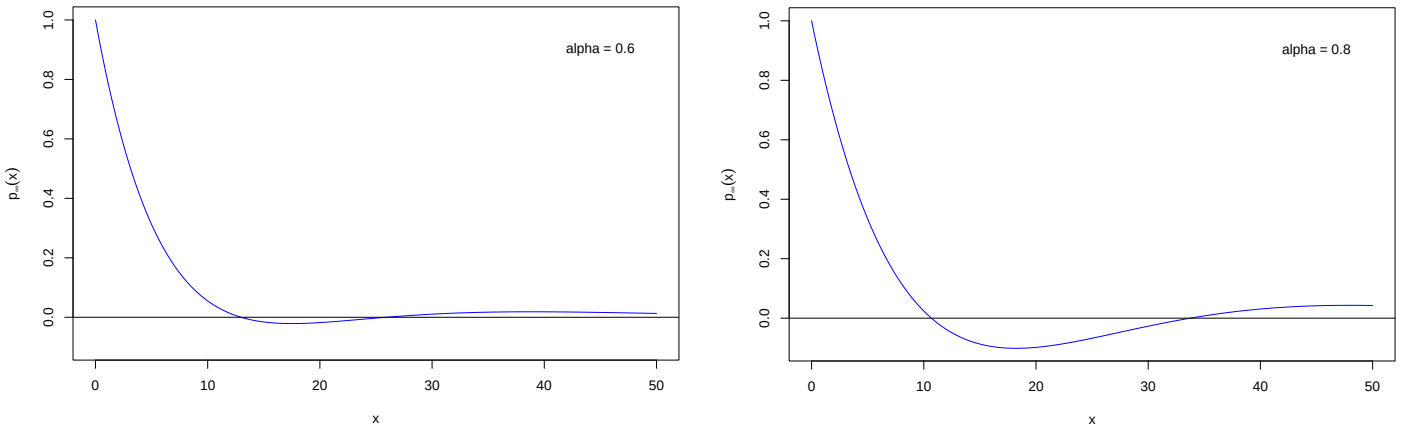


Figure 7. Plots of $p_\infty(x)$ for $\alpha = 0.6$ and $\alpha = 0.8$ as functions of the dimensionless argument x. In both cases the curve crosses the horizontal axis, showing that p_∞ has a positive root for these values of α. From the mechanical viewpoint, this implies that the fractional model predicts a critical buckling load in this regime.

To compare the fractional model with the classical Euler theory, it is convenient to introduce the normalized critical load

$$\frac{P_\alpha}{P_{\text{cl}}} = \frac{\Gamma(2-\alpha)\, s_0(\alpha)}{\pi^2/4},$$

where $P_{\text{cl}} = \frac{EI\pi^2}{4l^2}$ denotes the classical Euler critical load corresponding to the case $\alpha = 1$. This dimensionless quantity isolates the contribution of the fractional parameter and makes explicit how the critical load predicted by the model varies with α. In particular, the fractional formulation exhibits not only quantitative differences with respect to the classical case, but also a qualitative threshold behavior: for the values discussed in this section, no positive root exists when $\alpha \leq 0.526$, and therefore the model does not predict a critical load in that regime.

Table 3 shows that, for the sample values considered here, the ratio P_α / P_{cl} increases as α decreases. This indicates that the fractional parameter has a strong influence on the buckling threshold within the present formulation, and suggests that α may serve as an effective index for distinguishing different buckling responses predicted by the model.

Table 3. Normalized critical load P_α / P_{cl} for selected values of the fractional parameter α.

α	Approximation of $s_0(\alpha)$	P_α/P_{cl}
1	$\pi^2/4$	1.0000
0.7	11.45145302	4.1653
0.6	12.97715518	4.6665
0.527	17.30961111	6.2132

5. Conclusions

In this section, we will address the results obtained. Initially, we have deduced a formula for the radius of curvature that incorporates the fractional index $\alpha \in (0, 1]$. This formula has been pivotal in formulating our fractional model for column buckling. Subsequently, based on the hypothesis that a polynomial can accurately approximate the elastic curve, we have established the existence of a critical buckling force (Theorem 2). Furthermore, we have managed to calculate an approximation of this critical buckling force that, within a previously defined margin of error (Theorem 3), closely approaches the real force. We observe that for values of $\alpha \leq 0.526$, the critical force does not exist, while for $\alpha \geq 0.527$, it exists.

A more detailed sensitivity analysis of the transition region near $\alpha = 0.526$–0.527 could provide further insight into the threshold behavior observed in our numerical experiments; however, such an investigation lies beyond the scope of the present work and will be considered in future research.

An important area of opportunity is the exploration of alternative models for beam buckling. This is a vast field, as there are numerous ways in which a beam can buckle (see [17]). Moreover, for each model, different types of fractional derivatives (beyond the Caputo derivative) can be considered, allowing one to physically verify which derivative best captures the buckling behavior.

Expression (1) reveals substantial potential for diversification. By merely altering the curvature moment of the structure of interest, we can derive various fractional differential equations. This observation also suggests a broad range of potential applications. As noted in the Introduction, these curvature-based formulations are relevant to the stability problems arising in civil and aerospace engineering, for example. Although the present work is conceptual, these directions illustrate the practical relevance of the proposed framework and motivate future developments.

It is important to acknowledge several limitations of this study. The first is that the equipment required for the physical validation of the fractional model is very expensive, at least for us. However, other researchers may have access to such equipment or the necessary resources to continue developing our work. The second limitation is theoretical: the initial approximations to s_0 are determined by graphically analyzing the roots of the polynomials p_{even} (see Assumption 1).

Author Contributions: Conceptualization, J.V.-M.; methodology, J.V.-M. and M.R.-A.; formal analysis, J.V.-M. and M.R.-A.; investigation, J.V.-M.; resources, J.V.-M. and M.R.-A.; writing—review and editing, J.V.-M. and M.R.-A.; visualization, J.V.-M. and M.R.-A.; supervision, J.V.-M. All authors have read and agreed to the published version of the manuscript.

Funding: The authors J.V.-M. and M.R.-A. received partial support from grants PIM25-2 and PIM23-6, respectively, from the Universidad Autónoma de Aguascalientes.

Data Availability Statement: This study is purely conceptual and does not utilize specific empirical data.

Acknowledgments: To the referees for their careful review of the manuscript.

Conflicts of Interest: The authors declare no conflicts of interest.

References

1. Kumar, S.; Kumar, R.; Agarwal, R.P.; Samet, B. A study of fractional Lotka–Volterra population model using Haar wavelet and Adams–Bashforth–Moulton methods. *Math. Methods Appl. Sci.* **2020**, *43*, 5564–5578. [CrossRef]
2. Hilfer, R. *Applications of Fractional Calculus in Physics*; World Scientific: Singapore, 2000.
3. Debnath, L. Recent applications of fractional calculus to science and engineering. *Int. J. Math. Math. Sci.* **2003**, *2003*, 3413–3442.
4. Karniadakis, G.E. (Ed.) *Handbook of Fractional Calculus with Applications*; Numerical Methods; De Gruyter: Berlin, Germany; Boston, MA, USA, 2019; Volume 3.
5. Lin, S.-D.; Srivastava, H.M. Some miscellaneous properties and applications of certain operators of fractional calculus. *Taiwan. J. Math.* **2010**, *14*, 2469–2495. [CrossRef]
6. Diethelm, K.; Garrappa, R.; Giusti, A.; Stynes, M. Why fractional derivatives with nonsingular kernels should not be used. *Fract. Calc. Appl. Anal.* **2020**, *23*, 610–634. [CrossRef]
7. Becerra-Guzmán, G.; Villa-Morales, J. Erroneous applications of fractional calculus: The catenary as a prototype. *Mathematics* **2024**, *12*, 2148. [CrossRef]
8. Martínez-Jiménez, L.; Cruz-Duarte, J.M.; Rosales-García, J.J. Fractional solution of the catenary curve. *Math. Methods Appl. Sci.* **2021**, *44*, 7969–7978.
9. Conejero, J.A.; Franceschi, J.; Picó-Marco, E. Fractional vs. ordinary control systems: What does the fractional derivative provide? *Mathematics* **2022**, *10*, 2719. [CrossRef]
10. Ortigueira, M.D. A coherent approach to non-integer order derivatives. *Signal Process.* **2006**, *86*, 2505–2515. [CrossRef]
11. Domokos, G.; Holmes, P.; Royce, B. Constrained Euler buckling. *J. Nonlinear Sci.* **1997**, *7*, 281–314. [CrossRef]
12. Wang, C.M.; Wang, C.Y. *Exact Solutions for Buckling of Structural Members*; CRC Press: Boca Raton, FL, USA, 2004; Volume 6.
13. Luo, A.C.J.; Hamidzadeh, H.R. Equilibrium and buckling stability for axially traveling plates. *Commun. Nonlinear Sci. Numer. Simul.* **2004**, *9*, 343–360. [CrossRef]
14. Failla, G.; Zingales, M. Advanced materials modelling via fractional calculus: Challenges and perspectives. *Philos. Trans. Ser. A Math. Phys. Eng. Sci.* **2020**, *378*, 20200050. [CrossRef] [PubMed]
15. Sidhardh, S.; Patnaik, S.; Semperlotti, F. Fractional-order structural stability: Formulation and application to the critical load of nonlocal slender structures. *Int. J. Mech. Sci.* **2021**, *201*, 106443. [CrossRef]
16. Spiegel, M.R. *Applied Differential Equations*; Pearson: New York, NY, USA, 1980.
17. Timoshenko, S.P.; Gere, J.M. *Theory of Elastic Stability*; McGraw-Hill: New York, NY, USA, 1961.
18. Ortigueira, M.; Machado, J. Which derivative? *Fractal Fract.* **2017**, *1*, 3. [CrossRef]
19. Diethelm, K. *The Analysis of Fractional Differential Equations*; Lecture Notes in Mathematics; Springer: Berlin/Heidelberg, Germany, 2010; Volume 2004.
20. Kilbas, A.A.; Srivastava, H.M.; Trujillo, J.J. *Theory and Applications of Fractional Differential Equations*; North-Holland Mathematics Studies; Elsevier: Amsterdam, The Netherlands, 2006; Volume 204.
21. Samko, S.G.; Kilbas, A.A.; Marichev, O.I. *Fractional Integrals and Derivatives: Theory and Applications*; Gordon and Breach Science Publishers: Yverdon, Switzerland, 1993.

Disclaimer/Publisher's Note: The statements, opinions and data contained in all publications are solely those of the individual author(s) and contributor(s) and not of MDPI and/or the editor(s). MDPI and/or the editor(s) disclaim responsibility for any injury to people or property resulting from any ideas, methods, instructions or products referred to in the content.